Title
A covalent organic framework onion structure

Authors
Zheng, Qi
Li, Xinle
Zhang, Qiubo
et al.

Publication Date
2022-11-01

DOI
10.1016/j.mattod.2022.09.002

Peer reviewed

Deciphering Nitrogen-rich Covalent Organic Framework Onion Structure at the Atomic Level

Qi Zheng[1,2], Xinle Li[3#], Qiubo Zhang[1], Daewon Lee[1,4], Karen C. Bustillo[3], Yi Liu[3], Jinyang Jiang[2], Haimei Zheng[1,4]*

[1] Materials Sciences Division, Lawrence Berkeley National Laboratory, Berkeley, California 94720, United States
[2] School of Materials Science and Engineering, Southeast University, Nanjing 211189, P.R. China
[3] The Molecular Foundry, Lawrence Berkeley National Laboratory, Berkeley, California 94720, United States
[4] Department of Materials Science and Engineering, University of California, Berkeley, California 94720, United States

[#] Current address: Department of Chemistry, Clark Atlanta University, Atlanta, Georgia 30314, United States

[*] Corresponding authors: Haimei Zheng, hmzheng@lbl.gov

Abstract
Constructing and characterizing hierarchical nanomaterials such as onion nanostructures from the bottom up remains challenging. Herein, we report a closed-cage, onion-like structure of covalent organic framework (COF) obtained through a low-temperature solvothermal synthesis. Extensive transmission electron microscopy analysis revealed the atomic arrangement of this unique COF onion with embedded rich nitrogen in a periodic pyrazine-fused porous graphitic framework. The COF onion structure displayed aza-fused graphitic features in a complex stacking mode. Some defects in the form of five- or seven-member rings and the interlayer stacking faults can be essential to form such distinctive nanostructures. We constructed a corresponding model that predicts COF onion properties following experimental observations. This novel onion exhibited a bandgap value of 2.56 eV, resembling other carbon-based nanomaterials, suggesting potential applications in sensors, photocatalysts, and nanoelectronics.

Keywords
C-N nanomaterials; covalent organic framework (COF); onion structure; porous graphitic frameworks; transmission electron microscopy (TEM)

1. Introduction

Although graphite, with two-dimensional layers stacking together, is one of the stable forms of carbon under ambient conditions, at the nanometer scale, it forms zero-dimensional structures, such as graphene quantum dots,[1–3] fullerenes[4–7] , etc.[8,9] Such dimension reduction brings new opportunities to access unusual materials properties through the control of nanostructures.[10–13] This virtue is not limited to carbon, and, in recent years, onion-like structures have been made from numerous compounds with layered two-dimensional nanostructures.[14–16] For instance, onion-like structures derived from layered two-dimensional nanostructures have incurred great interest in the formation mechanism and structure-property relationships.

Covalent organic frameworks (COFs) are crystalline porous polymers integrating organic units into extended periodic networks with atomic precision.[18–20] 2D COFs are obtained by covalently assembling the organic monomeric units in the desired geometry.[21,22] Due to the hybridized states (sp, sp^2, sp^3) of carbon[23–25] with diverse bonding in the COF structure, complex nanostructures, such as spheres,[26–28] belts,[29] or microtubes,[30] have been achieved. These complex nanostructures possess properties that differ significantly from their bulk counterparts with layered 2D structures. Considering the exceedingly designable architecture and versatile applications of COFs, the controllable synthesis of COF-based nanostructures is of prime importance. COF onion structures, made from metal-free, purely organic-based 2D frameworks, may incur new insight into the formation mechanism and the material properties compared to their counterparts made of inorganic 2D layers. The synthesis and characterization of such COF onions are, however, unprecedented and need to be explored.

In this work, a novel carbon-nitrogen (C-N) COF onion was obtained through a facile low-temperature solvothermal process. We identified its structure and deciphered its layer stacking features via transmission electron microscopy (TEM). Advanced chemical mapping coupled with electron energy-loss spectroscopy (EELS) was employed to determine the elemental and atomic bonding characters. The onion structure is highly nitrogenous with distinct graphitic features in a complex stacking mode. The novel C-N COF onion presents a bandgap at ~2.6 eV owing to its intrinsic sp^2 hybridized conjugated skeletons. We expect broad applications of these COF onions, such as in sensors, catalysts, and electronics.

2. Results and Discussions

2.1. Identification of a novel C-N COF onion

We previously developed a facile method for synthesizing 2D pyrazine-fused PGF-1 (porous graphitic framework, PGF).[31]. The reversible condensation of 1,2,4,5-benzenetetramine (BTA) tetrahydrochloride and hexaketocyclohexane (HKH) octahydrate under basic hydrothermal conditions produced highly crystalline PGF-1 (**Figure S1**). By selecting the suitable solvent (N-Methyl-2-Pyrrolidone, NMP) coupled with optimal centrifuge procedures, we successfully separated the phases and discovered a novel C-N COF onion.

Onion-like nanostructures exist in many materials commonly known as 2D layered structures, such as graphene,[32–34] BN,[35,36] MoS_2,[37–39] WS_2,[40,41] Cs_2O,[42] etc.[43–45] Most of these syntheses involve high-temperature or high-pressure processes, such as flaming, solar ablation, or detonation. Controllable fabrication of onion-like nanostructures in a mild condition is of considerable scientific interest and has not been achieved previously.

Similar to traditional carbon onions, our COF onion consists of concentric shells in a polyhedral shape (**Figure 1a**). In **Figure 1b**, these 2D layers possess highly fused aromatic backbones, periodic nanopores (~1.2 nm), and π-stacking columns with an interlayer stacking distance of approximately 0.33 nm, which is distinctly different from the other reported onion-like nanostructures. We found that the COF onions have a uniform size from 20 to 30 nm (**Figure 1c**) and a central void in most individual particles. Different porosity can be attained by adjusting the void size. There is a tendency for the shell thickness to decrease with a larger void (**Figure 1d**). For example, the shell is 9 nm when the central void is 3.2 nm, compared with a 4 nm shell grown on a 5.5 nm void. This is presumably governed by the minimization of surface energy.[46] Although the onion particles display different features, the measured *d* spacing between two adjacent layers remains the same as 0.33 nm (**Figure 1e**), which agrees with the interlayer distance of bulk COFs (**Figure S2**).

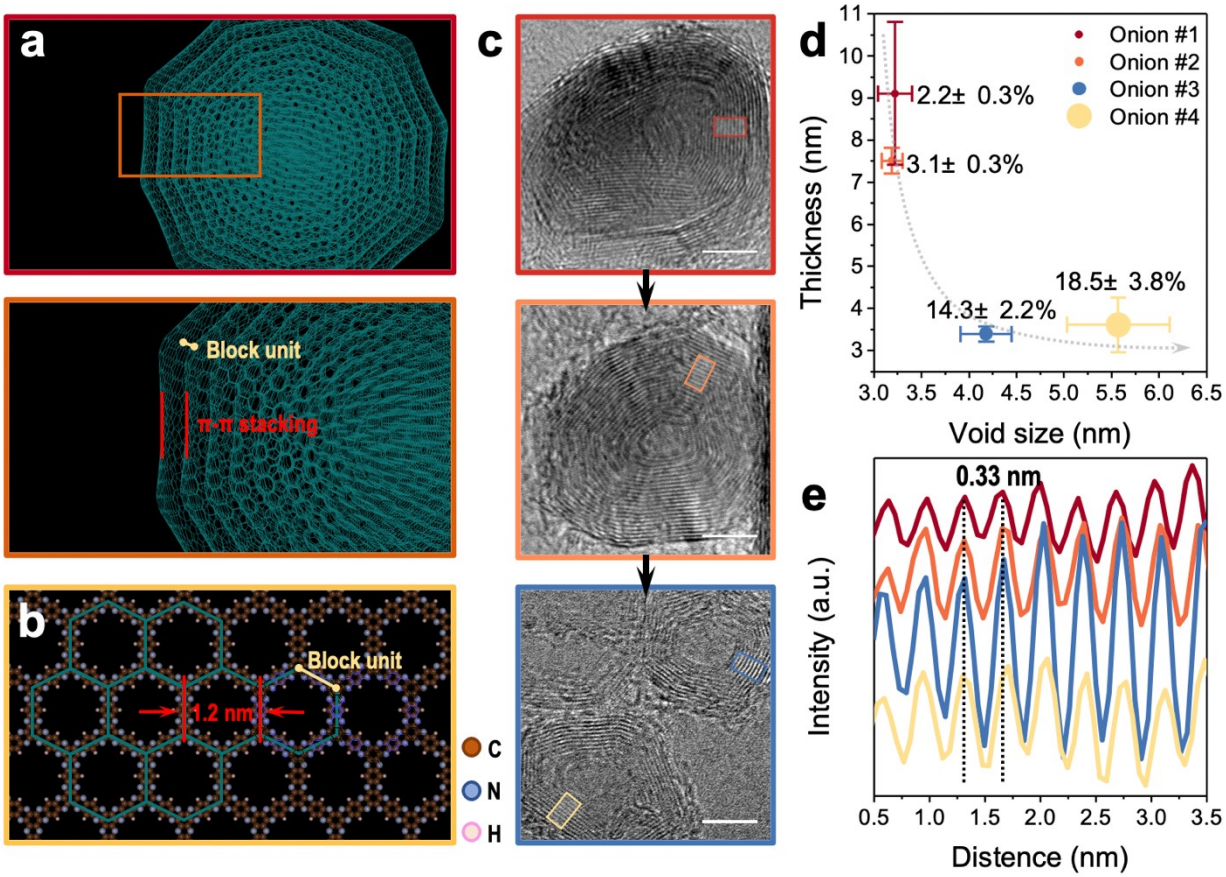

Figure 1. Discovery of COF onion. (**a**) Illustration on a COF onion at different scales. Concentric shells with an interlayer spacing of 0.33 nm can be observed. (**b**) The COF onion is

composed of aza-fused aromatic backbones with well-arranged 1.2 nm pores. (**c**) High resolution transmission electron microscopy (HRTEM) images of four representative COF onions. The onion exhibits a "void-shell" structure with graphite-like shells. Scale bars, 5 nm. (**d**) The relation between the void size and shell thickness in different onions (the color is consistent with the border color in (**c**)). The porosity (the ratio between the void and the whole onion, calculated by projected area) of the onion is labeled along with data points. The error bar is estimated by multiple calculations. (**e**) The distance between the two layers is calculated at 0.33 nm in the highlighted regions in (**c**).

2.2. Elemental and bonding structure of C-N COF onions

Highly concentrated COF onions were achieved through an optimal centrifuge procedure and were illustrated in **Figure 2a** (see method for details). We observed that the onions display graphitic layers at a 0.33 nm spacing indicated by the inserted FFT pattern. The surface electrostatic potential is relatively high considering the nanosize effect of onion particles, which induces the aggregation of COF onions. Similar clustering phenomena have been reported in other carbon-based materials such as nanodiamonds.[47] We performed a quantitative analysis on the COF onion aggregates (**Figure 2b**) and found that the particles exhibit an average size of 5.7 nm, including a 1.7 nm graphitic shell. Geometrically, the onions are primarily convex with a polydispersity from 0.4 to 0.8 in the circularity. The average aspect ratio is estimated at 1.8, representing an oval shape of onion aggregates.

According to the energy dispersive spectroscopy (EDS) mapping in **Figure 2c**, both carbon and nitrogen elements are uniformly distributed in the COF onions. A rich nitrogen composition up to ~25% (At) was detected (**Figure S3**). As each BTA molecule contains 4 nitrogen atoms, the COF onion structure is fully decorated with nitrogen, in the formula of $(C_5N_2H_1)_n$. This is also consistent with the results from the full spectrum in **Figure 2d**.

The Fourier transform infrared (FTIR) spectrum (**Figure S4**) shows the characteristic pyrazine stretching bands at 1238 cm^{-1}.[48] Different from amorphous nitrogen-doped systems,[49,50] we have achieved a unique nitrogenous onion structure with ordered atomic arrangements. ^{13}C cross-polarization magic angle spinning (^{13}C-CP/MAS) NMR spectroscopy (**Figure S4**) further confirmed the formation of pyrazine linkages. The ^{13}C-CP/MAS NMR spectrum showed resonances signaled at 108, 134, and 142 ppm, which could be assigned to the pyrazine carbon atoms adjacent to the nitrogen atoms, carbon atoms of the hexaazatrinaphthalene nodes on vertices, and the unsubstituted carbon atoms of the phenyl edge, respectively.[51]

We applied electron energy-loss spectroscopy (EELS) to study the interatomic bonding of the COF onions. Carbon and nitrogen are evaluated as the main chemical composition in the COF onions (**Figure 2d**). The sharp N K-edge, which doesn't exist in the background region, excludes the artifacts from carbon film as the COF onion sample is drop-casted on the ultrathin carbon-supported copper grid. The pronounced peak at ~20 eV in the low loss spectrum (**Figure 2e**) was assigned to the $\pi+\sigma$ plasmon owing to the collective oscillation of π and σ valence electrons.[52] Another peak at 6.5 eV is the sign of π plasmon from the sp^2 bonding in the COF onion, which is common in graphite or other sp^2- carbon-based materials.[53] We further examined near-edge fine

structures between carbon-nitrogen linkages. In detail, the peak at 286.8 eV represents 1s→π* transitions of sp^2 carbon while the main edge at ~297 eV is due to 1s→σ* transitions from sp^3 bonds.[54,55] It is common that sp^3 carbon single bonds remain in COFs due to the structural defects.[56] Similarly, the nitrogen peak at 396.8 eV is ascribed to 1s→π* transition.[57] This strong nitrogen π* peak indicated significant nitrogen in sp^2-bonded aromatic rings in the form of a pyridine structure.[58,59] The findings in EELS confirm that carbon and nitrogen in COF onions are in characteristic sp^2 bonding, which is consistent with the structure shown in **Figure 1**.

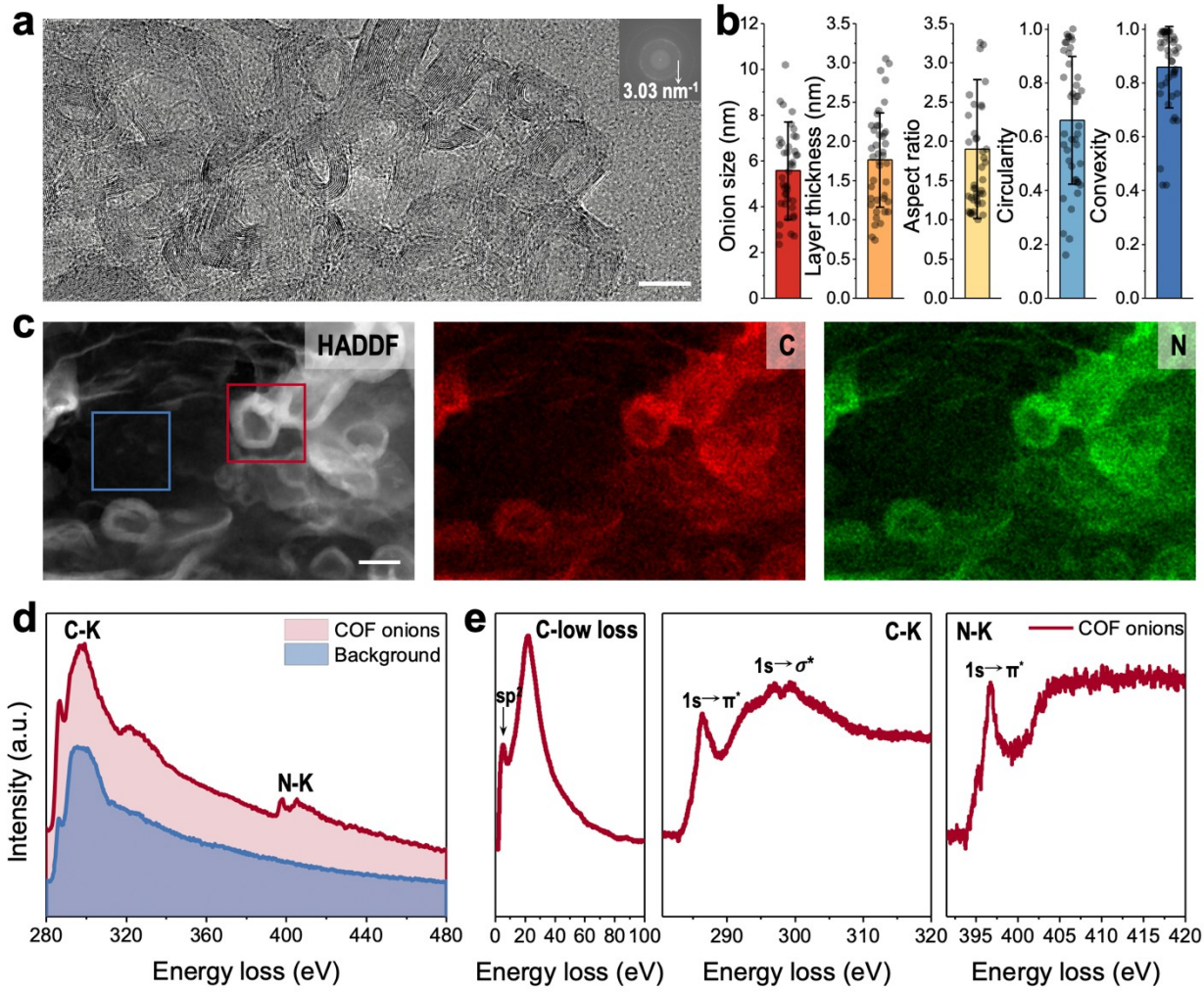

Figure 2. The structural and elemental information of COF onions. (**a**) COF onions with an interlayer spacing of 0.33 nm. Scale bar, 10 nm. Inserted is its corresponding FFT pattern. (**b**) Structure parameters of COF onions, including size, shell thickness, aspect ratio, circularity, and convexity, were calculated from (**a**). The entire frame TEM image can be found in **Supporting Information**, as well as definitions of the parameters and calculation formulas. Each dot represents one measurement, and the error bar is the standard deviation from the sampling. (**c**) Elemental mapping of COF onions. STEM-HADDF image and EDS maps of carbon (red) and nitrogen (green). Two regions with or without onions are highlighted in boxes for further EELS measurements in (**d**). Scale bar, 50 nm. (**d**) EELS spectra of COF onions and carbon film

background. (**e**) Low loss spectrum of C with an sp^2 peak distinguishable. The zero-loss line and the double scattering contributions are subtracted from the data. Near-edge structure of the C K-edge and N K-edge after individual subtraction of an inverse-power-law background.

2.3. Stacking modes of C-N COF onion layers

In **Figure 3a**, each graphitic layer in the onion was traced and color-coded by its local curvature. The result indicates that the onion is a polyhedron, and its terraces possess higher curvature values. More specifically, the COF onion particle shows a five-fold symmetry. It exhibits inherent characters: the region in the inner shell at a high curvature value may result in the outer shell region becoming much curled accordingly. The evidence manifests the possible mechanism of onion growth through layer-by-layer attachment. The onion structure was also confirmed by the simulated TEM image in **Figure 3b** (also see **Figure S5**). The further tomographic analysis supports a real 3D onion structure by a series of tilting (**Figure S6**).

The radial intensity profile in **Figure 3c** exhibits three prominent diffraction peaks. The broad peak at 0.12 $Å^{-1}$ can be assigned to the (100) facet, representing the front view of the structure with hexagonally arranged pores of 1.2 nm. According to structural simulations with different stacking configurations, the (001) at 0.3 $Å^{-1}$ corresponds to the π-π stacking of onion layers.[60,61] Moreover, the peak at the spacing of 2.1 Å is consistent with the size of the aromatic pyrazine ring.[31] In **Figure 3d**, the local interlayer spacing of 2D layers was captured (see more details in **Supporting Information**). Van der Waals interactions are predominated between the onion layers, and we found significant heterogeneity in the stacking. As expected, the surface layers share a larger interlayer spacing up to 0.5 Å, attributed to the surface strain-induced reconstruction.[62] Defects or dislocations can also cause different stacking configurations. For example, some local regions such as the onion corners, boundaries, and terraces (see arrows in **Figure 3d**) also exhibit localized expansion. A bimodal distribution of interlayer spacing is noted in **Figure 3e**. The first peak at 0.33 nm is the normal stacking, while the peak at 0.37 nm is caused by the stacking distortion from the surfaces and boundaries.[63] The layer stacking mode is complicated. Here, we postulate a model including AA, AB, and SP (saddle point) stacking considering the large variety of interlayer spacing obtained. The heterogeneous stacking of layers can be the inherent mechanism for forming onion structure through flexible non-planar conformation since abundant stacking faults can be commonly distinguished in the COF onions (**Figure 3f**).

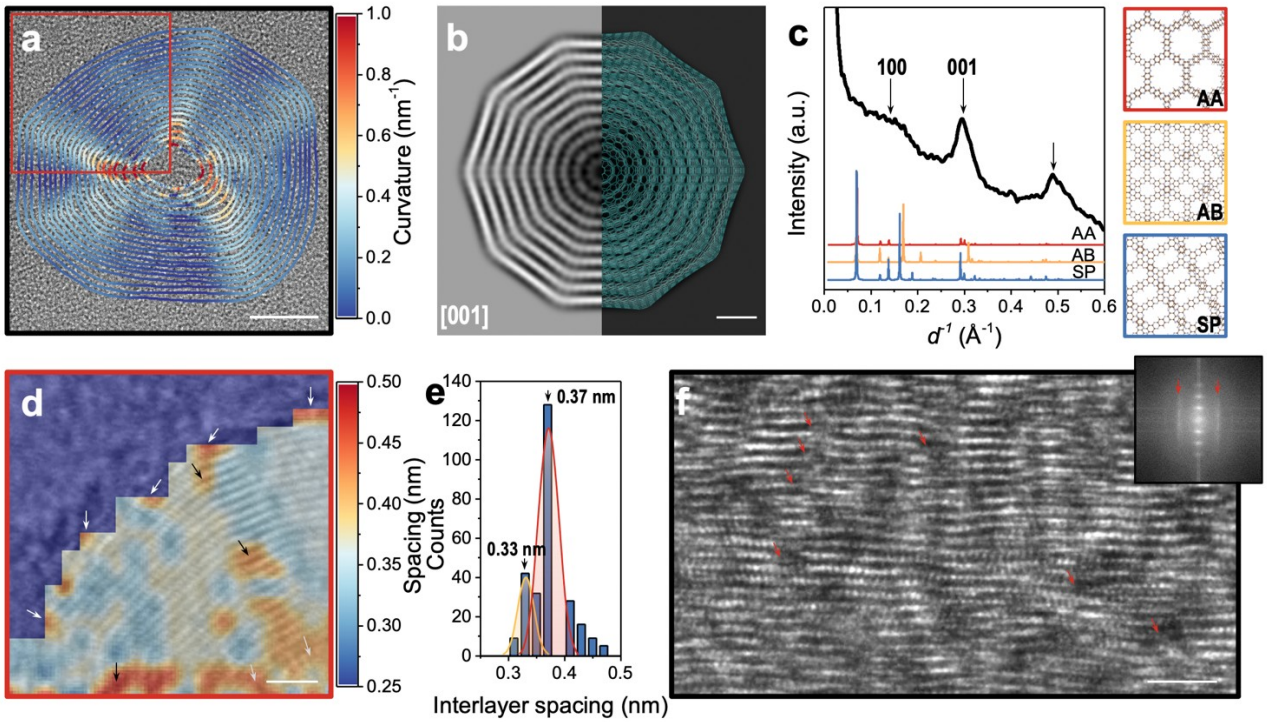

Figure 3. Layer stacking modes in COF onion. (**a**) Map of the graphitic layers in the onion structure color-coded by the local curvature. Scale bar, 5 nm. The original TEM image and detailed image analysis method can be found in **Supporting Information**. (**b**) Multi-slice TEM simulation on a polyhedron onion, observed from the [001] perspective. Scale bar, 1 nm. (**c**) Radial intensity profile of COF onion derived from the diffraction. Some peaks can be assigned to certain facets according to diffraction simulations on different stacking modes of COF layers. (**d**) Mapping the interlayer spacing of the COF onion based on the magnified region in (**a**). Scale bar, 2 nm. The spacing is calculated by the partitioned FFT analysis based on 10x10 proportion step with an overlap of 10 pixels. More details can be found in **Supporting Information**. (**e**) Distribution of the interlayer spacing, fitted using Gaussian functions. (**f**) Heterogeneity of layer stacking in the onion structure. Defects and stacking faults are highlighted by arrows. Scale bar, 2 nm. The inserted is the corresponding FFT pattern, showing streaking due to stacking faults.

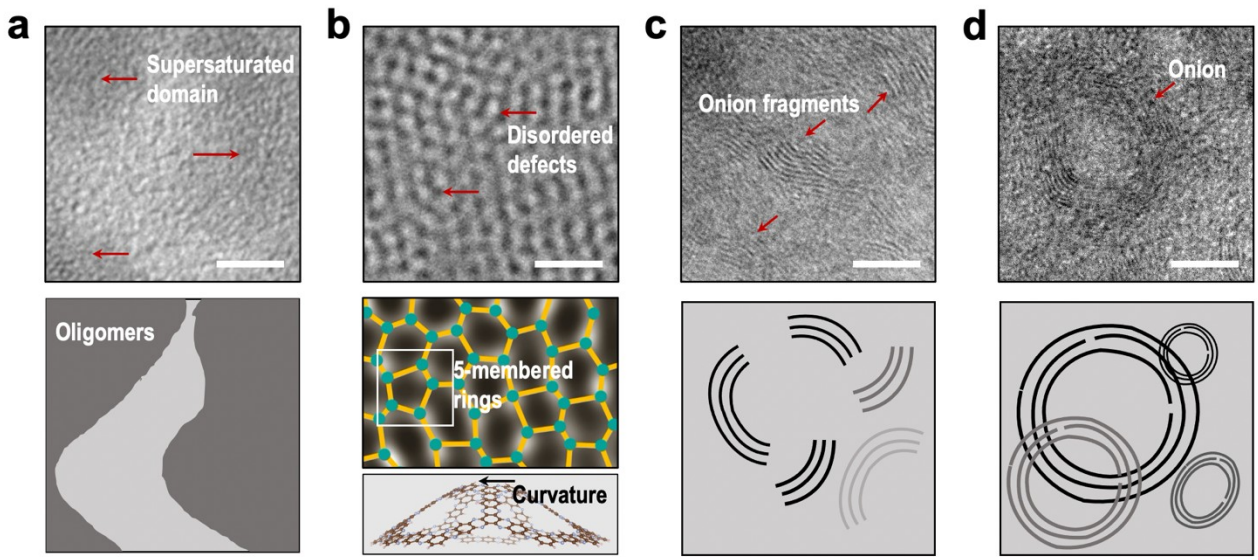

Figure 4. Schematic representation of the process of crystallization and formation of COF onions. Four stages including (**a**) Supersaturated aqueous solution with oligomers (dark regions); (**b**) Formation of the graphitic nucleus with defects during the polymerization (bottom inserted: mishap of connectivity that cause the loss of in-plane order); (**c**) Growth and (**d**) layer thickening of the onion nanoparticles. Scale bars, 5 nm.

Traditional onion-like nanostructures, including graphene onions, MoS_2 onions are generated using high-temperature/ high-pressure processes. Such methods provide high-intensity shockwaves and cause local heterogeneity in the system, which leads to heterogeneous nucleation and growth. We proposed that the formation of COF onions is also controlled by the nanoscale heterogeneity and fluctuations in the basic aqueous solution (**Figure 4**).[64]

In detail, an initial solution containing oligomers can be produced upon the dissolution of BTA and HKH precursors in water. Then, the COF layers nucleate from the supersaturated aqueous solution. Because defects occur during condensation, these graphitic layers tend to fold to minimize surface energy. For example, some of the COF flocs may contain five- or seven-membered macrocyclic rings that can be stabilized as curved structures after sufficient structural optimization (**Figure S7**). These cone-like structures can be the intermediates in the formation of COF onions. Note that the different defects can alter the shape of onions from spherical to oval ones, leading to onions of varying sizes and circularities. This also explains the heterogeneity of onion aggregates in **Figure 2**. Consequently, the COF onions may grow layer by layer to form the nested layered nanostructure.

We proposed a perfect COF onion belonging to the icosahedral family (**Figure S8**, also see detailed construction methods in **Supporting Information**).[65] Note that different onion models can be constructed based on the geometry criterion.[66,67] Our COF onion model consists of 12 pentagonal rings and hexagonal ones in a certain number, which can be calculated using Euler's theorem. The hexagonal rings in the center are in a planar configuration, while the pentagonal rings at vertices bend in an inward longitudinal curvature. These pentagons can provoke the

curving of the COF nucleus into a bowl-shaped structure and thus zip up its open edges, ending up with a closed onion structure during the crystallization process.[17]

2.4. Optical properties of COF onions

Furthermore, we investigated the optical properties of COF onions for their potential applications. Direct UV-Vis measurement shows a broad absorption (**Figure 5a**) with an optical bandgap of 2.5 eV, which is similar to fullerenes (**Figure 5b**).[68] The COF onion is surprisingly stable and deforms at a high yield strength, without crack propagation from the fracture according to our molecular dynamics simulation (**Figure S9**). The exceptional plasticity of this COF onion could be useful in nanoscopic pressure cells[69,70] and flexible electronics.[71,72] Some other applications such as porous hosts for drug delivery,[73] high-capacity cathodes for batteries,[31] and electrocatalysts are also highlighted (**Figure S10**).[74,75]

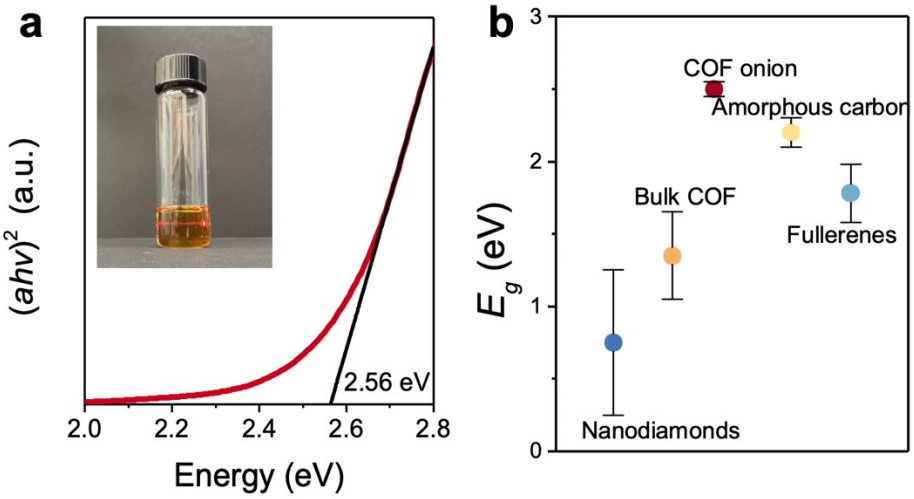

Figure 5. Optical properties of COF onions. (**a**) Tauc plot calculated using an absorption coefficient α and photon energy hv (h, Planck constant; v, frequency) to determine the optical bandgap of COF onions. Extrapolating the linear region (red line) estimates an optical bandgap of 2.5 eV. Inset, the Tyndall effect confirms the colloidal nature of COF onions dispersions. (**b**) Comparison of the bandgap of COF onions against different carbon-based materials, including fullerenes,[68,76] nanodiamonds,[77,78] monolayer amorphous carbon,[79] and the bulk COF nanomaterial.[31] The error bar is estimated from the measurements.

3. Conclusions

In summary, we have successfully synthesized a novel COF onion nanostructure through a facile hydrothermal synthesis. This COF onion contains orderly arranged carbon and nitrogen in the aza-fused skeletons, and the size can also be controlled with an average size of 5.7±1.2 nm. The structure of the COF onion is resolved by atomic-resolution TEM imaging and spectroscopy, which reflect its graphitic layered feature and long-range periodicity. Defects, dislocations, and stacking faults are also observed, which account for the formation of such exquisite nanostructures. The COF onion exhibits an optical bandgap similar to other carbon-based nanomaterials, indicating its significant potential in energy storage and catalysis applications.

This work reveals insightful information regarding the atomic features of COF onion structures and informs our understanding of their growth mechanisms.

4. Experimental details

Preparation of COF onions. 1,2,4,5-benzenetetramine tetrahydrochloride (BTA, 12.8 mg, 0.045 mmol) and hexaketocyclohexane octahydrate (HKH, 9.3 mg, 0.030 mmol) were dissolved in water (2 ml) in a 5 ml-Biotage vial. Note that 45 µl 4 M potassium hydroxide solution was added as the catalyst. Then, the mixture was degassed by freeze-pump-thaw for three cycles and sealed under vacuum. The vial was heated in an oven at 120 °C for 3 days. Finally, the precipitates were collected by centrifugation and filtration, washed with water and methanol. The precipitates were re-dispersed in N-Methyl-2-Pyrrolidone (NMP) and sonicated for 60 min at 30 °C (**Figure S11**). To separate the COF onions (~20 nm) from the large bulk samples (~µm), we further centrifuged the dispersion at 10,000 rpm for 10 min (**Figure S12**). The supernatant containing COF onions was kept and concentrated. Then the onion sample was drop-casted onto a copper grid (Ultrathin C on lacey, 300 mesh Cu) for further TEM characterization.

TEM characterization. TEM images were acquired using a ThemIS transmission electron microscope with a Thermo Fisher Scientific Ceta CMOS camera. The microscope was operated at 300 keV with the Bruker SuperX energy dispersive x-ray spectroscopy (EDS) detector, allowing rapid chemical identification. Electron energy loss spectroscopy (EELS) analysis was performed on FEI Tecnai F20 UT at 200 kV in STEM mode with 0.15 eV energy resolution. The energy dispersion was set to 0.3 eV per channel for the full spectrum and 0.02 eV per channel for the near-edge structure of C and N K-edges.

UV-vis spectroscopy. The liquid-state UV-vis absorbance measurement was performed on Cary 5000 UV-Vis-NIR spectrometer, from 180 to 1000 nm at the step of 1 nm.

Supporting Information

Supporting Information is available from the Wiley Online Library or from the author.

Acknowledgments

This work was supported by the U.S. Department of Energy (DOE), Office of Science, Office of Basic Energy Sciences (BES), Materials Science and Engineering Division under Contract No. DE-AC02-05-CH11231 within the KC22ZH program. J. Jiang acknowledges the support from the National Natural Science Foundation of China (No. 51925903) and the National Key R&D Program of China (2018YFC0705401). Work at the Molecular Foundry is supported by the Office of Science, Office of Basic Energy Sciences, of the U.S. Department of Energy under Contract No. DE-AC02-05CH11231.

Received: ((will be filled in by the editorial staff))

Revised: ((will be filled in by the editorial staff))

Published online: ((will be filled in by the editorial staff))

References

[1] B. Trauzettel, D. V Bulaev, D. Loss, G. Burkard, *Nat. Phys.* **2007**, *3*, 192.
[2] M. Bacon, S. J. Bradley, T. Nann, *Part. Part. Syst. Charact.* **2014**, *31*, 415.
[3] Y. Yan, J. Gong, J. Chen, Z. Zeng, W. Huang, K. Pu, J. Liu, P. Chen, *Adv. Mater.* **2019**, *31*, 1808283.
[4] H. W. Kroto, J. R. Heath, S. C. O'Brien, R. F. Curl, R. E. Smalley, *Nature* **1985**, *318*, 162.
[5] W. Krätschmer, L. D. Lamb, K. Fostiropoulos, D. R. Huffman, *Nature* **1990**, *347*, 354.
[6] K. Kikuchi, N. Nakahara, T. Wakabayashi, S. Suzuki, H. Shiromaru, Y. Miyake, K. Saito, I. Ikemoto, M. Kainosho, Y. Achiba, *Nature* **1992**, *357*, 142.
[7] R. Taylor, D. R. M. Walton, *Nature* **1993**, *363*, 685.
[8] P. Shemella, Y. Zhang, M. Mailman, P. M. Ajayan, S. K. Nayak, *Appl. Phys. Lett.* **2007**, *91*, 42101.
[9] K. Kamalasanan, R. Gottardi, S. Tan, Y. Chen, B. Godugu, S. Rothstein, A. C. Balazs, A. Star, S. R. Little, *Angew. Chemie Int. Ed.* **2013**, *52*, 11308.
[10] M. Li, Y. Yang, Z. Wang, T. Kang, Q. Wang, S. Turren-Cruz, X. Gao, C. Hsu, L. Liao, A. Abate, *Adv. Mater.* **2019**, *31*, 1901519.
[11] J. Wei, C. Ding, P. Zhang, H. Ding, X. Niu, Y. Ma, C. Li, Y. Wang, H. Xiong, *Adv. Mater.* **2019**, *31*, 1806197.
[12] Q. Wu, L. Yang, X. Wang, Z. Hu, *Adv. Mater.* **2020**, *32*, 1904177.
[13] A. Aubele, Y. He, T. Kraus, N. Li, E. Mena-Osteritz, P. Weitz, T. Heumüller, K. Zhang, C. J. Brabec, P. Bäuerle, *Adv. Mater.* **2021**, 2103573.
[14] R. Tenne, *J. Mater. Res.* **2006**, *21*, 2726.
[15] R. Tenne, M. Redlich, *Chem. Soc. Rev.* **2010**, *39*, 1423.
[16] B. Višić, L. S. Panchakarla, R. Tenne, *J. Am. Chem. Soc.* **2017**, *139*, 12865.
[17] A. Chuvilin, U. Kaiser, E. Bichoutskaia, N. A. Besley, A. N. Khlobystov, *Nat. Chem.* **2010**, *2*, 450.
[18] A. P. Cote, A. I. Benin, N. W. Ockwig, M. O'Keeffe, A. J. Matzger, O. M. Yaghi, *Science* **2005**, *310*, 1166.
[19] H. M. El-Kaderi, J. R. Hunt, J. L. Mendoza-Cortés, A. P. Côté, R. E. Taylor, M. O'Keeffe, O. M. Yaghi, *Science* **2007**, *316*, 268.
[20] T. Ma, E. A. Kapustin, S. X. Yin, L. Liang, Z. Zhou, J. Niu, L.-H. Li, Y. Wang, J. Su, J. Li, *Science* **2018**, *361*, 48.
[21] N. Huang, P. Wang, D. Jiang, *Nat. Rev. Mater.* **2016**, *1*, 16068.
[22] Y. Jin, Y. Hu, W. Zhang, *Nat. Rev. Chem.* **2017**, *1*, 1.
[23] K. Kaiser, L. M. Scriven, F. Schulz, P. Gawel, L. Gross, H. L. Anderson, *Science* **2019**, *365*, 1299.
[24] E. Jin, M. Asada, Q. Xu, S. Dalapati, M. A. Addicoat, M. A. Brady, H. Xu, T. Nakamura, T. Heine, Q. Chen, *Science* **2017**, *357*, 673.
[25] L. Zhu, G. M. Borstad, H. Liu, P. A. Guńka, M. Guerette, J.-A. Dolyniuk, Y. Meng, E. Greenberg, V. B. Prakapenka, B. L. Chaloux, *Sci. Adv.* **2020**, *6*, eaay8361.
[26] S. Kandambeth, V. Venkatesh, D. B. Shinde, S. Kumari, A. Halder, S. Verma, R. Banerjee, *Nat. Commun.* **2015**, *6*, 1.
[27] W. Ma, Q. Zheng, Y. He, G. Li, W. Guo, Z. Lin, L. Zhang, *J. Am. Chem. Soc.* **2019**, *141*,

18271.
[28] Y.-Y. Liu, X.-C. Li, S. Wang, T. Cheng, H. Yang, C. Liu, Y. Gong, W.-Y. Lai, W. Huang, *Nat. Commun.* **2020**, *11*, 1.
[29] S. Wan, J. Guo, J. Kim, H. Ihee, D. Jiang, *Angew. Chemie Int. Ed.* **2008**, *47*, 8826.
[30] B. Gole, V. Stepanenko, S. Rager, M. Grüne, D. D. Medina, T. Bein, F. Würthner, F. Beuerle, *Angew. Chemie Int. Ed.* **2018**, *57*, 846.
[31] X. Li, H. Wang, H. Chen, Q. Zheng, Q. Zhang, H. Mao, Y. Liu, S. Cai, B. Sun, C. Dun, *Chem* **2020**, *6*, 933.
[32] P. R. Buseck, S. J. Tsipursky, R. Hettich, *Science* **1992**, *257*, 215.
[33] N. Sano, H. Wang, M. Chhowalla, I. Alexandrou, G. A. J. Amaratunga, *Nature* **2001**, *414*, 506.
[34] C. Liu, A. V Singh, C. Saggese, Q. Tang, D. Chen, K. Wan, M. Vinciguerra, M. Commodo, G. De Falco, P. Minutolo, *Proc. Natl. Acad. Sci.* **2019**, *116*, 12692.
[35] V. V Pokropivny, V. V Skorokhod, G. S. Oleinik, A. V Kurdyumov, T. S. Bartnitskaya, A. V Pokropivny, A. G. Sisonyuk, D. M. Sheichenko, *J. Solid State Chem.* **2000**, *154*, 214.
[36] C. Tang, Y. Bando, Y. Huang, C. Zhi, D. Golberg, *Adv. Funct. Mater.* **2008**, *18*, 3653.
[37] P. A. Parilla, A. C. Dillon, K. M. Jones, G. Riker, D. L. Schulz, D. S. Ginley, M. J. Heben, *Nature* **1999**, *397*, 114.
[38] M. Chhowalla, G. A. J. Amaratunga, *Nature* **2000**, *407*, 164.
[39] A. Zak, Y. Feldman, V. Alperovich, R. Rosentsveig, R. Tenne, *J. Am. Chem. Soc.* **2000**, *122*, 11108.
[40] Y. Golan, C. Drummond, M. Homyonfer, Y. Feldman, R. Tenne, J. Israelachvili, *Adv. Mater.* **1999**, *11*, 934.
[41] L. Rapoport, N. Fleischer, R. Tenne, *Adv. Mater.* **2003**, *15*, 651.
[42] A. Albu-Yaron, T. Arad, M. Levy, R. Popovitz-Biro, R. Tenne, J. M. Gordon, D. Feuermann, E. A. Katz, M. Jansen, C. Muehle, *Adv. Mater.* **2006**, *18*, 2993.
[43] J. Bai, A. V Virovets, M. Scheer, *Science* **2003**, *300*, 781.
[44] H.-J. Zhai, Y.-F. Zhao, W.-L. Li, Q. Chen, H. Bai, H.-S. Hu, Z. A. Piazza, W.-J. Tian, H.-G. Lu, Y.-B. Wu, *Nat. Chem.* **2014**, *6*, 727.
[45] O. Brontvein, A. Albu-Yaron, M. Levy, D. Feuerman, R. Popovitz-Biro, R. Tenne, A. Enyashin, J. M. Gordon, *ACS Nano* **2015**, *9*, 7831.
[46] H.-G. Liao, D. Zherebetskyy, H. Xin, C. Czarnik, P. Ercius, H. Elmlund, M. Pan, L.-W. Wang, H. Zheng, *Science* **2014**, *345*, 916.
[47] A. S. Barnard, E. Ōsawa, *Nanoscale* **2014**, *6*, 1188.
[48] C. Y. Zhang, J. M. Tour, *J. Am. Chem. Soc.* **1999**, *121*, 8783.
[49] Z. Xu, X. Zhuang, C. Yang, J. Cao, Z. Yao, Y. Tang, J. Jiang, D. Wu, X. Feng, *Adv. Mater.* **2016**, *28*, 1981.
[50] Z. Zhou, Y. Zhang, Y. Shen, S. Liu, Y. Zhang, *Chem. Soc. Rev.* **2018**, *47*, 2298.
[51] M. Karplus, J. A. Pople, *J. Chem. Phys.* **1963**, *38*, 2803.
[52] A. C. Ferrari, A. Libassi, B. K. Tanner, V. Stolojan, J. Yuan, L. M. Brown, S. E. Rodil, B. Kleinsorge, J. Robertson, *Phys. Rev. B* **2000**, *62*, 11089.
[53] M. Chhowalla, H. Wang, N. Sano, K. B. K. Teo, S.-B. Lee, G. A. J. Amaratunga, *Phys. Rev. Lett.* **2003**, *90*, 155504.

[54] P. Wesolowski, Y. Lyutovich, F. Banhart, H. D. Carstanjen, H. Kronmüller, *Appl. Phys. Lett.* **1997**, *71*, 1948.
[55] P. Redlich, F. Banhart, Y. U. Lyutovich, P. M. Ajayan, *Carbon N. Y.* **1998**, *36*, 561.
[56] O. Stephan, P. M. Ajayan, C. Colliex, P. Redlich, J. M. Lambert, P. Bernier, P. Lefin, *Science* **1994**, *266*, 1683.
[57] S. Waidmann, M. Knupfer, J. Fink, B. Kleinsorge, J. Robertson, *Diam. Relat. Mater.* **2000**, *9*, 722.
[58] M. Terrones, N. Grobert, H. Terrones, *Carbon N. Y.* **2002**, *40*, 1665.
[59] L. Laffont, M. Monthioux, V. Serin, R. B. Mathur, C. Guimon, M. F. Guimon, *Carbon N. Y.* **2004**, *42*, 2485.
[60] E. L. Spitler, B. T. Koo, J. L. Novotney, J. W. Colson, F. J. Uribe-Romo, G. D. Gutierrez, P. Clancy, W. R. Dichtel, *J. Am. Chem. Soc.* **2011**, *133*, 19416.
[61] B. T. Koo, W. R. Dichtel, P. Clancy, *J. Mater. Chem.* **2012**, *22*, 17460.
[62] B. H. Kim, J. Heo, S. Kim, C. F. Reboul, H. Chun, D. Kang, H. Bae, H. Hyun, J. Lim, H. Lee, *Science* **2020**, *368*, 60.
[63] C.-C. Chen, C. Zhu, E. R. White, C.-Y. Chiu, M. C. Scott, B. C. Regan, L. D. Marks, Y. Huang, J. Miao, *Nature* **2013**, *496*, 74.
[64] N. D. Loh, S. Sen, M. Bosman, S. F. Tan, J. Zhong, C. A. Nijhuis, P. Král, P. Matsudaira, U. Mirsaidov, *Nat. Chem.* **2017**, *9*, 77.
[65] Y. Noël, M. De La Pierre, C. M. Zicovich-Wilson, R. Orlando, R. Dovesi, *Phys. Chem. Chem. Phys.* **2014**, *16*, 13390.
[66] H. Terrones, M. Terrones, *J. Phys. Chem. Solids* **1997**, *58*, 1789.
[67] M. Terrones, G. Terrones, H. Terrones, *Struct. Chem.* **2002**, *13*, 373.
[68] M. D. Diener, J. M. Alford, *Nature* **1998**, *393*, 668.
[69] F. Banhart, P. M. Ajayan, *Nature* **1996**, *382*, 433.
[70] Q. Huang, D. Yu, B. Xu, W. Hu, Y. Ma, Y. Wang, Z. Zhao, B. Wen, J. He, Z. Liu, *Nature* **2014**, *510*, 250.
[71] Y. Sun, J. A. Rogers, *Adv. Mater.* **2007**, *19*, 1897.
[72] T. Cheng, Y. Zhang, W. Lai, W. Huang, *Adv. Mater.* **2015**, *27*, 3349.
[73] V. N. Mochalin, O. Shenderova, D. Ho, Y. Gogotsi, *Nat. Nanotechnol.* **2012**, *7*, 11.
[74] Z. Xiang, D. Cao, L. Huang, J. Shui, M. Wang, L. Dai, *Adv. Mater.* **2014**, *26*, 3315.
[75] L. Lin, Z. Lin, J. Zhang, X. Cai, W. Lin, Z. Yu, X. Wang, *Nat. Catal.* **2020**, *3*, 649.
[76] R. Pincak, V. V Shunaev, J. Smotlacha, M. M. Slepchenkov, O. E. Glukhova, *Fullerenes, Nanotub. Carbon Nanostructures* **2017**, *25*, 607.
[77] T. M. Willey, C. Bostedt, T. Van Buuren, J. E. Dahl, S. G. Liu, R. M. K. Carlson, R. W. Meulenberg, E. J. Nelson, L. J. Terminello, *Phys. Rev. B* **2006**, *74*, 205432.
[78] I. I. Vlasov, A. A. Shiryaev, T. Rendler, S. Steinert, S.-Y. Lee, D. Antonov, M. Vörös, F. Jelezko, A. V Fisenko, L. F. Semjonova, *Nat. Nanotechnol.* **2014**, *9*, 54.
[79] C.-T. Toh, H. Zhang, J. Lin, A. S. Mayorov, Y.-P. Wang, C. M. Orofeo, D. B. Ferry, H. Andersen, N. Kakenov, Z. Guo, *Nature* **2020**, *577*, 199.

Deciphering Nitrogen-rich Covalent Organic Framework Onion Structure at the Atomic Level

Qi Zheng[1,2], Xinle Li[3#], Qiubo Zhang[1], Daewon Lee[1,4], Karen C. Bustillo[3], Yi Liu[3], Jinyang Jiang[2], Haimei Zheng[1,4]*

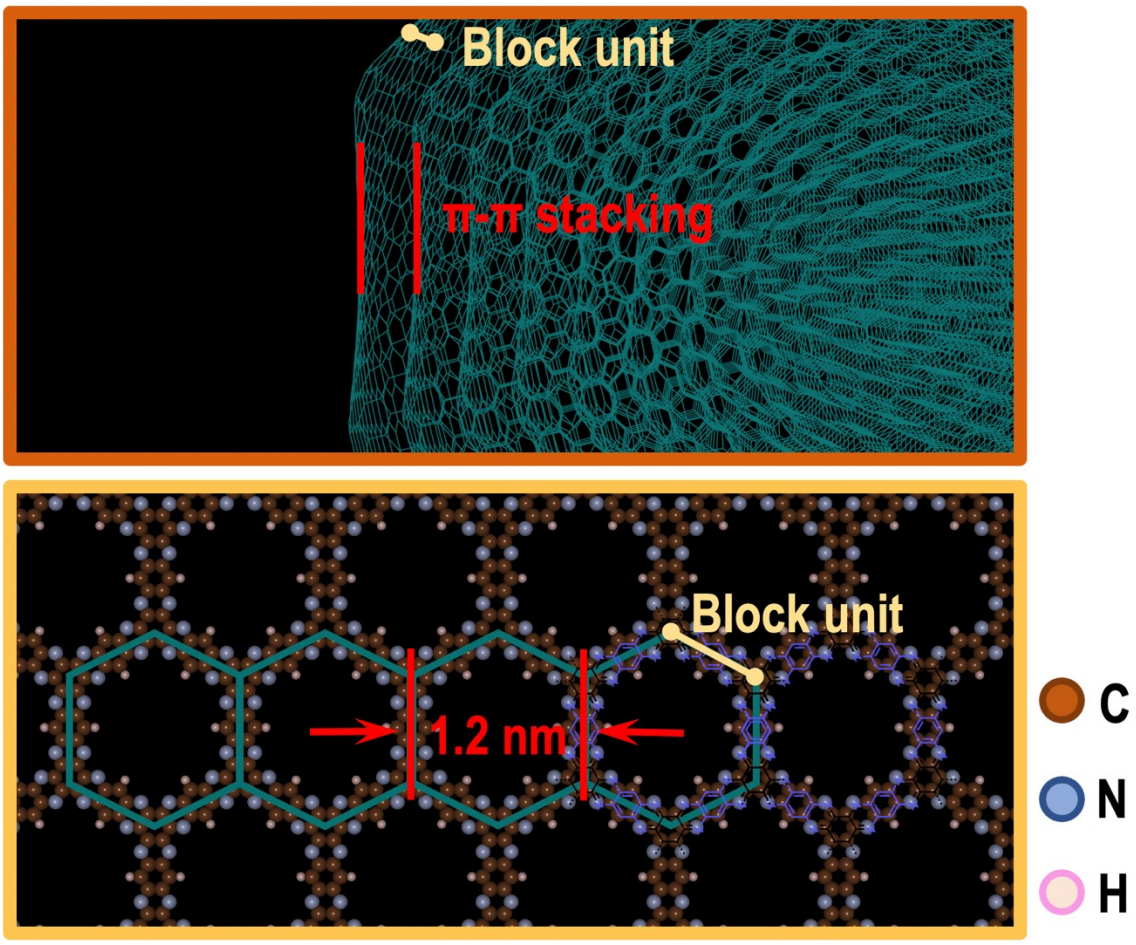

This paper demonstrates a low-temperature solvothermal method of nitrogen-rich covalent organic framework (COF) onions. The atomic structure and the bonding features are revealed by high resolution transmission electron microscopy (TEM) and electron energy-loss spectroscopy (EELS). The novel COF onion provides potential applications in batteries and catalysts.